

Article

# Big Data Analysis of the Speed Performance of a 176k DWT Bulk Carrier in Real Operating Conditions

Yurim Cho <sup>1</sup>  and Inwon Lee <sup>2,3,\*</sup> 

<sup>1</sup> Deep Ocean Engineering Research Center, Korea Research Institute of Ships & Ocean Engineering, Busan 46729, Republic of Korea; yusung49@naver.com

<sup>2</sup> Department of Naval Architecture and Ocean Engineering, Pusan National University, Busan 46241, Republic of Korea

<sup>3</sup> Global Core Research Center for Ships and Offshore Plants, Pusan National University, Busan 46241, Republic of Korea

\* Correspondence: inwon@pusan.ac.kr; Tel.: +82-51-510-2764

**Abstract:** Assessment of ship performance under in-service conditions is challenging due to the complex effects of many environmental disturbances. ISO 15016 and ISO 19030 standards are commonly used to evaluate ship operating performance. However, ISO 15016 requires numerous variables, a complex calculation formula, and considerable time and cost, and ISO 19030 only evaluates the reduction of ship speed caused by wind and neglects the effect of waves. To improve both standards and achieve a more accurate ship performance assessment, this study proposes a new performance prediction model, the multi-input single-output (MISO) system, which assumes that each ship has specific frequency characteristics according to type and size. Based on this new model, in-service navigation data collected from a 176k DWT bulk carrier, which amount to 5.7 million data points, are analyzed to assess the speed performance of the vessel subject to environmental disturbances. The proposed model was validated by comparing its results with ISO 19030 and specifically assessing the speed–power curves and speed reduction measured in operational data with the influence of environmental disturbances removed.

**Keywords:** ship speed performance; operational data; dynamic model; multi-input/single-output (MISO) system



**Citation:** Cho, Y.; Lee, I. Big Data Analysis of the Speed Performance of a 176k DWT Bulk Carrier in Real Operating Conditions. *J. Mar. Sci. Eng.* **2024**, *12*, 1816. <https://doi.org/10.3390/jmse12101816>

Received: 8 September 2024

Revised: 7 October 2024

Accepted: 9 October 2024

Published: 11 October 2024



**Copyright:** © 2024 by the authors. Licensee MDPI, Basel, Switzerland. This article is an open access article distributed under the terms and conditions of the Creative Commons Attribution (CC BY) license (<https://creativecommons.org/licenses/by/4.0/>).

## 1. Introduction

The severity of climate change has become a global concern, significantly affecting the global maritime community. In 2023, the International Maritime Organization (IMO) adopted the 2050 Net-Zero strategy. There have come into effect various regulations such as the EEDI (Energy Efficiency Design Index), EEXI (Energy Efficiency eXisting Ship Index), and CII (Carbon Intensity Index) rating systems. This represents a significant strengthening of energy efficiency regulations for existing ships as well as newbuilt ships. In order to meet these regulations, a variety of energy-saving methods for ships have been adopted. With the growing interest in the economic operation and associated new techniques, there has arisen a high demand for accurate predictions of performance variations for competitive ship navigation management. To achieve this, the use of ship operational big data analysis technology to assess ship external forces and improve predictive methods for fuel consumption and operational efficiency is essential. Since the 2010s, ship performance monitoring systems have been automated and computerized, and accumulate vast amounts of operational data. Based on these data, the analysis of the impact of external forces experienced during operation aids in understanding the causes behind performance variations. The use of ship operational big data analysis technology has prompted the need for analyzing the assessment of ship external forces and predictive methods for fuel consumption and operational efficiency.

The most important challenge in this regard is the accurate estimation of fuel consumption, which has significant impact on environment, the economy, and regulatory compliance [1–3]. Conventional methods of fuel consumption estimation mainly relied on on-board measurement data and statistical models, which show inadequacy in tracking the highly stochastic nature of marine environment and operational characteristics [4–6]. The fuel consumption of ocean-going vessels is affected by a variety of variables such as weather conditions, sea currents, and route specifics [7–9].

The physics-based method tries to offer a deterministic means of approximating fuel consumption based on specific assumptions [10]. Tillig and Ringberg [11] suggested a fuel consumption prediction model based in an energy systems theory. Recently, Kim et al. [12] proposed a comprehensive methodology consisting of ship resistance estimation and propulsion efficiency.

Data-driven and/or machine learning approaches encompass various aspects, such as research on big data preprocessing methods and the development of performance prediction models based on machine learning. There have been reported several review papers discussing the potential application of machine learning to predict the ship fuel consumption [5,13,14]. Regarding big data preprocessing, the process of variable selection previously relied heavily on experience. However, there is now a growing trend in conducting research based on correlation analysis between variables, leading to more diverse approaches. Petersen et al. [15] proposed a fuel consumption prediction model by performing principal component analysis (PCA) in the data preprocessing stage to understand the relationships between variables. They used artificial neural networks and Gaussian processes to develop the model. Shin et al. [16] created an approximation model using mathematical models by analyzing the sensitivity between the collected data to assess the impact of each variable. Yoo and Kim [17] also developed prediction models for engine output and speed based on the relationships between known physical systems of ships using regression analysis. As the amount of data becomes extensive and the prediction based on general ship mechanical relationships reaches its limits, research on performance prediction using machine learning is actively pursued. Kim et al. [18] compared their prediction model using the Support Vector Machine (SVM) algorithm with the ISO 15016 [19] method. Karagiannidis et al. [20] proposed a method of processing ship operation data and developed an artificial intelligence model aimed at reducing the carbon emissions of ships. Wahl [21] presented a technique to predict the fuel consumption of ships in transit, taking into account external environmental factors such as currents, winds, and waves. Uyanik et al. [22] performed a machine learning study to predict the fuel consumption of a ship based on the ship engine data. Gupta et al. [23] applied such machine learning methods as principal component regression (PCR), partial least squares regression (PLSR), and artificial neural network (ANN) to analyze the hydrodynamic performance of sea-going ships. Abebe et al. [24] proposed a machine learning approach using the Automatic Identification System (AIS) to predict ship speed; they also compared their deep learning model to the ISO 19030 method to predict the increase in speed loss due to fouling.

A detailed inspection of the above-mentioned literature, however, indicates that the accurate and reliable assessment of the performance of a ship in real operating conditions has rarely been presented. Ocean-going vessels are ceaselessly exposed to environmental disturbances such as wind, waves, and currents. The random nature of such disturbances gives rise to random added resistance and added power. In real practice, ships are mainly operated at a constant engine speed and power, and the speed of the ship fluctuates by the balance between the power supply from the engine and the varying power demand due to the disturbances. Consequently, the ship speed has a large amount of scatter at constant power, which is contrary to the well-defined speed–power relationship obtained from a model test or sea trial. In real operating conditions, engine power should be regarded as the input and speed as the output. However, most of the existing literature maintains the classic speed–power relationship, which attempts to predict power consumption at a given

speed. That is one of the major hindrances to a reliable assessment of ship performance in actual operating conditions.

In this study, improvements were made to address the limitations of previous research. Firstly, we did not rely on ISO standard models or regression methods based on ship mechanical relationships. Instead, our study pursued the correct, reversed causality in real operating conditions, as shown in Figure 1. In other words, we propose a dynamic model by which the correct speed can be predicted at measured shaft power and the analysis of environmental disturbances. Secondly, we designed a prediction model that considers the dynamic characteristics of a ship during operation, taking into account the influence of external forces. The ISO 19030 standard calculates speed variations using performance values (PV) and treats the effect of disturbances statically by excluding dynamic effects. However, our study considered the dynamic effects of a ship's navigation conditions where external forces such as relative wind speed and wave height fluctuate (increase). As a result, wind resistance, wave resistance, and other forces increase accordingly and cause variations in speed performance. We assumed that there were frequency characteristics (time delays) about the time constant of the ship, which varies based on the size and type of the ship, and we interpreted these time constants. Thirdly, in the data interpretation process, we opted to use most of the operational data without extensive preprocessing such as filtering, except for the minimal removal of outliers (e.g., berthing data and data with excessive speed change) in contrast to the practice based on the ISO 19030 standard reported by Cho et al. [25].

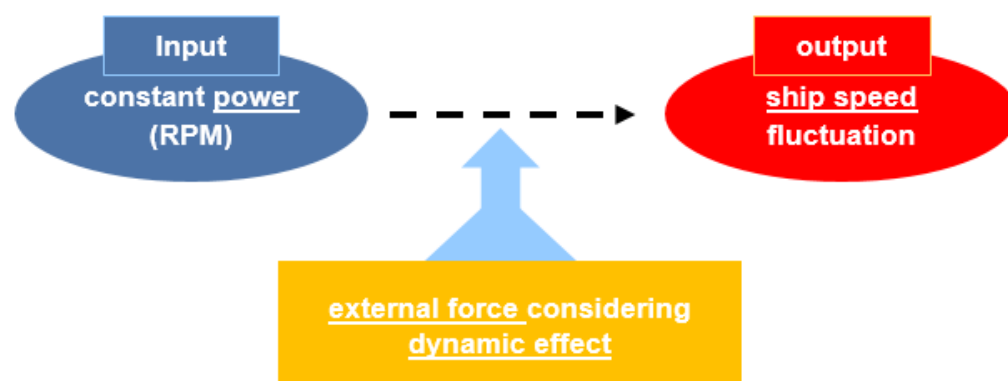


**Figure 1.** Concept of the operating performance estimation model.

Based on the above assumptions, a novel multi-input single-output (MISO) linear dynamic response model is established to identify factors that influence ship speed performance degradation through correlation analysis between external forces and speed in real sea states. In addition, we propose a performance prediction model that quantifies the impact of each variable on speed performance by isolating each impact. While the existing ISO 19030 standard can only assess speed performance degradation for a specific ship, the present model, which considers the characteristics of real sea states, can preclude the influences of environmental disturbances. This permits a more reasonable assessment of ship performance and, thus, the comparison of performances between different ships. With these improvements over existing research and standards, we present an enhanced performance assessment model for ships in real operating conditions. It is also worth mentioning that the present ship speed performance model could be integrated into a more comprehensive model for the ships with an unconventional propulsion system or autonomous control system. Exemplary models have been developed by Boychuk et al. [26] and Zwierzewicz et al. [27].

The organization of the paper is as follows: Section 2 describes the shortcomings of the existing ISO standards for ship performance assessment; Section 3 formulates the new analysis model devised in this study and provides detailed information on the vessel and operational data.; Section 4 describes how the new dynamic model is configured to

analyze the input–output relationship between environmental disturbances and speed fluctuations. Section 5 presents the main results obtained from the study’s MISO linear dynamic response model and compares them with those from the existing ISO 19030 standard. Section 6 discusses the main findings and implications of the present study. Finally, Section 7 provides the main conclusions.

## 2. Improvement of ISO Standard

Various models based on actual operation data for ship performance prediction are being proposed. In the past, ship performance prediction relied on non-standardized analysis methods, leading to frequent disputes between designers and shipowners. To standardize ship performance prediction, ISO 19030 standard [28,29] has been established and has undergone several revisions, and is widely used. The authors’ previous papers [25,30] also evaluated performance based on ISO 19030. While ISO standards provide a standardized interpretation based on test results for fundamental aspects, there is still room for improvement. Therefore, research on the improvement of ISO 19030 standard and the proposal of new models using machine learning for big data analysis are actively conducted in the field of ship performance prediction. The objective of this study is also to identify improvement points in existing research and propose new models for the enhancement of ship performance prediction in actual operating conditions.

The ISO 19030 standard explains the general principles for measuring changes in hull and propeller performance and defines a set of performance indicators for hull and propeller maintenance, repair, and retrofit activities. It employs the method of correcting the collected data for wind resistance and filtering to obtain the propulsion power corrected to calm sea conditions and defines the ship’s performance by comparing the expected speed with the measured ship speed difference. It provides detailed explanations of data preprocessing and force-correction methods, making it a user-friendly standard, but there are some areas for improvement, including the following:

- Correction for External Forces: While ISO 19030 considers the influence of wind, it does not account for the effects of waves and currents. As a result, the interpretation of performance is done with the inclusion of wave and current effects, making it challenging to compare the performance of different vessels. However, it allows for the comparison of the same vessel’s hull and propeller performance over time with the intention to measure performance changes for a specific vessel, as specified in the ISO 19030 standard.
- Preprocessing of Operational Data: Preprocessing operational data according to the ISO 19030 standard involves dividing the data into 10 min blocks and applying Chauvenet filtering to major operational data such as speed through water, speed over ground, and RPM. However, this filtering process can lead to a significant amount of data, ranging from 30% to 70%, being filtered out due to environmental factors. This raises concerns about whether the performance analysis results can be considered representative of the vessel’s entire operational range [31]. Figure 2 shows the application of data filtering before and after according to the ISO 19030 standard for the first voyage of the target vessel (approximately two weeks). The blue points represent the data distribution over the previous two-week period. However, as evident from the plot, many data points deviate from the clustered data. Such data points are filtered out through two rounds of filtering, leaving only the valid data points represented by green diamond shapes, which are used for interpretation. Consequently, the blue dots and orange crosses represent the data filtered during the preprocessing and this filtered portion is roughly estimated to be approximately 70% in this particular sample.

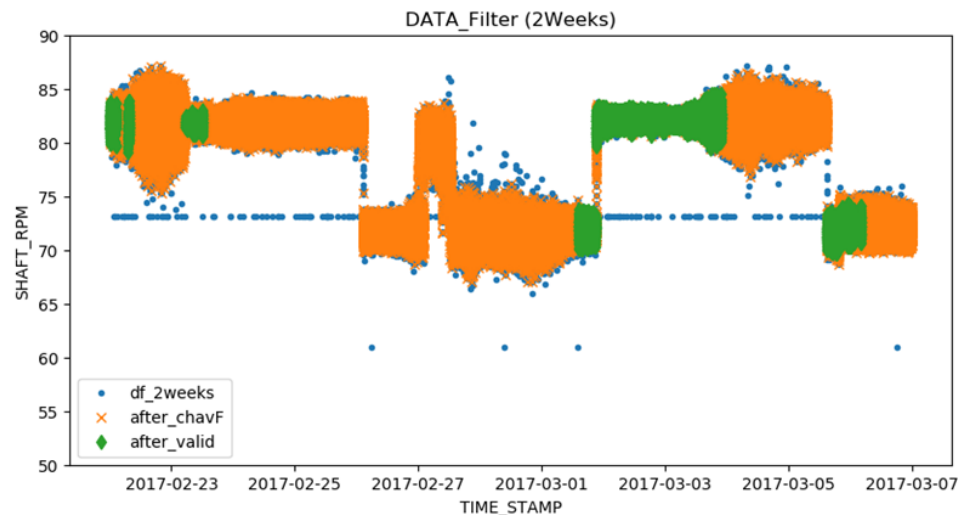


**Figure 2.** Sample plot of measured data and validated data for 2 weeks.

### 3. Materials and Methods

#### 3.1. Multi-Input, Single-Output (MISO) Linear Dynamic Response Model

In the preceding section, we raised the issue that a new performance prediction model needs to reduce the excessive data loss due to over-filtering during the preprocessing stages. The main objective of this new model is to analyze the impact of interconnected marine forces on a component-wise basis and reduce data loss. To achieve this, the proposed model takes a more dynamic approach to the analysis. It considers the varying effects of maritime forces, such as relative wind speed and wave height, during actual operations. By doing so, the model aims to minimize the data loss caused by excessive filtering and provides a more comprehensive understanding of how these forces influence vessel performance. The fundamental concept is based on the general notion that changes in external forces during actual vessel operations, such as relative wind speed and wave height, result in added resistance, including wind resistance and wave resistance, which in turn, leads to variations in the vessel's speed over ground (SOG). Additionally, the proposed model assumes the existence of frequency characteristics, represented by time constants, associated with the size and type of the target vessel.

Real operational data are not only vast in quantity but also contain a wealth of information, making their analysis very complicated. Therefore, for the analysis of operational data, we propose a prediction model based on the data interpretation technique presented by Bendat and Piersol [32]. This technique involves transforming the measured input/output data into the frequency domain and identifying the optimal linear system between the input and output. We have modeled the unknown frequency characteristics of various variables that affect the vessel's speed performance as a linear multi-input single-output (MISO) system. By determining the optimal linear transfer function between the input variables and the output, we can calculate speed performance variations without the influence of environmental variables. This dynamic model is distinct from the traditional static model because it takes into account the time-varying nature of the vessel's speed performance and eliminates the effects of environmental variables. The general MISO model for arbitrary inputs is shown in Figure 3a. Here, the  $X_i(f)$ ,  $i = 1, 2, \dots, q$  term represents the Fourier transformation of the input variables  $X_i(t)$ . The linear frequency response function is denoted by  $H_{iy}(f)$ , and the unknown external output noise in the ideal model is represented by  $N(f)$ . The concept of the model for ordered conditional inputs in Figure 3a is illustrated in Figure 3b. The Fourier transformations  $X_i \sim X_q$  are computed sequentially for input variables. The input variables are not interrelated, and the expression for input Fourier transformation  $X_i(f)$ ,  $i = 1, 2, \dots, q$  indicates that the linear effect of  $X_{i-1}(t)$  has been removed from  $X_i(t)$  by the optimal linear system.

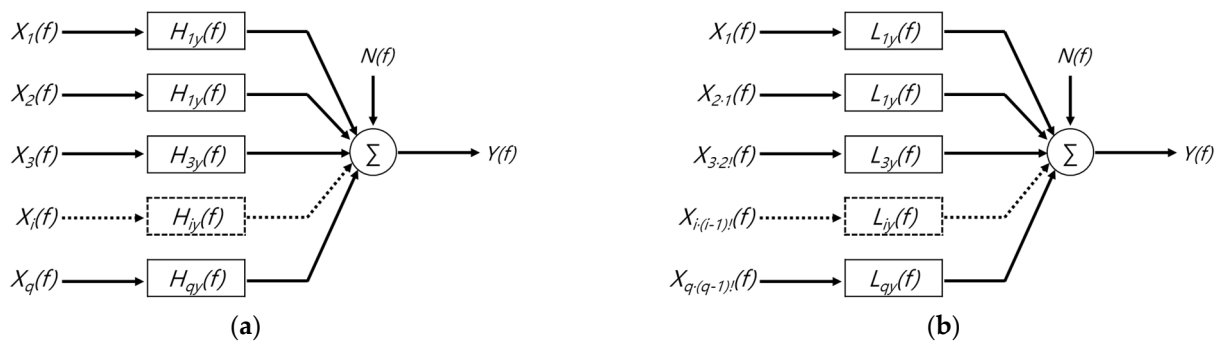


**Figure 3.** Multi-input, single-output (MISO) model: (a) general model for arbitrary inputs; (b) modified model for ordered conditioned inputs.

The present study defines a performance prediction model for one ship speed output with three external force inputs. As shown in Equation (1) and Figure 4, the model was defined to sequentially remove the influence of each force and observe the speed variation for each variable. It is worthwhile to mention that Equation (1) and Figure 4 are detailed representations of Figure 1, indicating how the external forces due to environmental fluctuations affect the ship speed in dynamic manner.

$$Y(f) = L_{1y}X_1 + L_{2y}X_{2.1} + L_{3y}X_{3.2!} + N \tag{1}$$

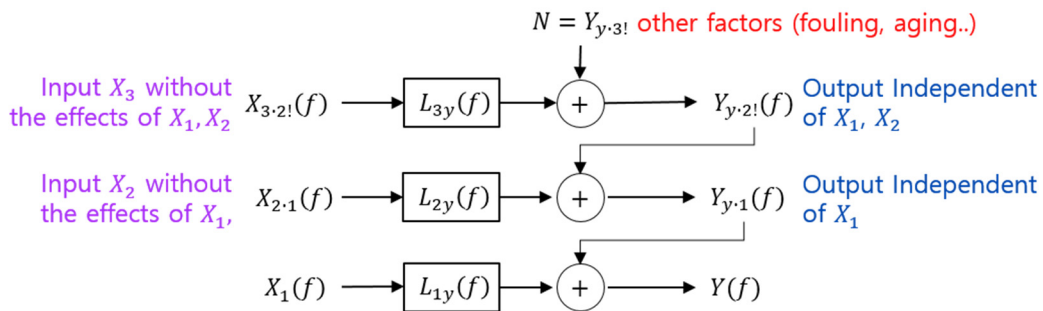


**Figure 4.** Multiple-input model for ordered conditioned inputs (three inputs and single output).

For the interpretation of Equation (1), the relevant equations are as follows:  $G$  is the spectral density function, where  $G_{ii}$  represents the auto-spectrum, and  $G_{ij}$  represents the cross-spectrum.  $L_{iy}$  in Equation (4) is the optimal transfer function. As a result, each linear system  $L_{iy}$  is defined as the ratio of the cross-spectral density function between the input and output to the auto-spectral density function of the input. When expressed as linear systems for each input variable, it can be represented as Equations (5)–(8). The last term on the right-hand side of Equation (1),  $N$ , represents the spectrum when calculated as a non-linear term unrelated to each input. It accounts for speed performance degradation factors other than external forces, such as fouling, aging, or any other causes that may lead to speed performance degradation in the analysis of ship performance data.

$$G_{ii} = \frac{2}{T}E[X_i^*X_i], \quad G_{ij} = \frac{2}{T}E[X_i^*X_j] \tag{2}$$

$$G_{iy} = \frac{2}{T}E[X_i^*Y] \tag{3}$$

$$L_{iy} = \frac{G_{iy \cdot (i-1)!}}{G_{ii \cdot (i-1)!}} \tag{4}$$

$$L_{1y} = \frac{G_{1y}}{G_{11}} = \frac{E[X_1^*Y]}{E[X_1^*X_1]}, \quad Y_{y,1} = Y - L_{1y}X_1 \tag{5}$$

$$L_{2y} = \frac{G_{2y.1}}{G_{22.1}} = \frac{E[X_{2.1}^* Y_{y.1}]}{E[X_{2.1}^* X_{2.1}]}, \quad Y_{y.2!} = Y_{y.1} - L_{2y} X_{2.1} \tag{6}$$

$$L_{3y} = \frac{G_{3y.2!}}{G_{33.2!}} = \frac{E[X_{3.2!}^* Y_{y.2!}]}{E[X_{3.2!}^* X_{3.2!}]}, \quad N = Y_{y.2!} - L_{3y} X_{3.2!} \tag{7}$$

$$X_{j.r!} = X_{j.(r-1)!} - L_{rj} X_{r.(r-1)!} \tag{8}$$

Here,  $X_1, X_{2.1}, X_{3.2!}$ , and  $X_{j.r!}$  represent the Fourier transforms of conditioned inputs. After the Fourier transforms  $Y(f), Y_{y.1}(f), Y_{y.2!}(f)$ , and  $N(f)$  are calculated from the nested calculations described in Equations (2)–(8) and Figure 4, the time histories of respective speed drops in time domain are obtained by inverse Fourier transform.

During operation, when external factors such as relative wind speed and wave height vary (increase), the resistance forces such as wind resistance and wave resistance also increase, causing fluctuations in the speed over ground (SOG). In this context, it is assumed that the time constant (time delay) associated with the size and type of the target vessel exists, which affects the frequency characteristics. The concept of the time constant is illustrated in Figure 5. The input transmitted is assumed to be a fixed random signal with zero mean value. Here,  $\alpha$  represents the constant attenuation factor,  $\tau_0$  is the constant time delay, and  $n(t)$  represents the noise in the output.

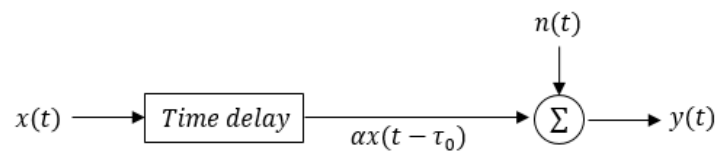


Figure 5. Model for time-delay problem.

### 3.2. Target Vessel

The vessel under consideration is a 176k DWT bulk carrier, whose principal particulars are provided in Table 1. This vessel operates regularly between Australia and South Korea as a bulk carrier. When traveling from Australia to South Korea, it operates in a “laden” condition with cargo on board, and when traveling from South Korea to Australia, it operates in a “ballast” condition with empty cargo holds. The voyages alternate between two ports, and each voyage period lasts approximately two weeks.

Table 1. Principal particulars of the 176k DWT bulk carrier.

Designation	Symbol	Value
Length overall	LOA	291.80 m
Breadth	B	45.00 m
Mean draft, laden condition	$T_L$	18.25 m
Mean draft, design condition	$T_D$	16.50 m
Mean draft, ballast condition	$T_B$	7.95 m

### 3.3. Operational Data

The operational data used in this study was automatically obtained by the Ship Performance Monitoring System (SPMS) installed on the 176k DWT bulk carrier since November 2014. The parameters of the automatic identification system (AIS) and weather data following the manner described in Abebe et al. [23] were automatically collected at 10 s intervals. The data sets in this study partly overlap those used in Cho et al. [24]. The analyzed data include information from three years after the first dry docking and approximately two years after the second dry docking. The main events and operational periods covered in the data range from November 2015 to November 2020. The entire data

set analyzed in this study contains approximately 5.7 million instantaneous data points. For more specific details, refer to Table 2. Table 3 shows the voyage information, average drafts, and acquired data during the second service period of approximately three years of operational data. The voyage information is based on the information provided by the shipping company.

**Table 2.** Key events and service periods for the 176k DWT bulk carrier.

Event	Time/Period	Voyage No.
SPMS installation	November 2014	
First dry docking	November 2015	
Second service period (3 years)	November 2015~November 2018	Ballast 38~64/laden 38~64
Second dry docking	December 2018	
Third service period (2 years)	January 2019~November 2020	Ballast 65~78/laden 65~78

**Table 3.** Voyage details (second service period).

Voyage	Loading Condition	Departure [YYYY-MM-DD]	Arrival [YYYY-MM-DD]	Mean Draft [m]	No. of Data
39	Ballast	2015-11-20	2015-11-21	8.65	10,571
	Laden	2015-12-07	2015-12-20	14.96	9429
39	Ballast	2015-12-25	2016-01-04	7.55	7406
	Laden	2016-12-25	2016-01-27	17.98	8119
....					
62	Ballast	2018-09-18	2018-10-02	7.93	114,163
	Laden	2018-10-10	2018-10-27	17.71	126,279
63	Ballast	2018-11-03	2018-11-18	8.29	84,592
	Laden	2018-11-19	2018-12-02	18.08	105,038

#### 4. Inputs and Outputs for the Dynamic MISO Model

##### 4.1. Data Preparation

Real operational data are not only vast in quantity but also contain a wealth of information, making their analysis very complex. Therefore, the inclusion of all the information may compromise the accuracy of data interpretation. However, excessive filtering may also lead to performance analysis that fails to capture the unique characteristics of the operational data. In many studies involving operational performance big data, the data preprocessing stage is considered essential, and complex steps for data filtering and variable selection are often performed. Aside from using ISO standards for filtering methods, expert judgment from performance analysts is also employed to filter out outliers. However, in this study, the proposed model did not apply additional preprocessing beyond filtering for mechanical anomalies and environmental factors based on ISO 19030 standards during the data collection phase. As a result, more than 80% of the collected operational data for the specific vessel were used for interpretation. While the disadvantage of having a large amount of operational data is the potential increase in interpretation time, the proposed predictive model, considering its limited number of interpretation variables, did not incur any penalties in terms of interpretation time compared to the ISO 19030 standard method, which requires multiple data for performance analysis.

#### 4.2. Selection of Independent Variable Using Correlation Analysis

The proposed multi-input single-output (MISO) model relies on carefully selecting the input variables. The input variables that affect the output variable, which is speed performance, were chosen based on the correlation analysis between the input variables and the output variable, speed over ground. The variables used in the correlation analysis were selected based on the key parameters of the ISO 19030 standard and feature extraction from Abebe et al. [23]. The six selected variables are relative wind speed, current speed (from hindcast data), calculated current speed (difference between the speed through water (STW) and the speed over ground (SOG)), wave height (from hindcast data), bow relative motion, and shaft horsepower. These variables were chosen to assess their correlation with the output variable, which is the SOG. Figure 6 displays the correlation coefficients of the six variables with the SOG. For each SOG, high positive and negative correlations are observed, indicating strong relationships. The correlation evaluation revealed that relative wind speed, calculated current speed (=STW – SOG), wave height, and shaft horsepower have high correlations with the speed over the ground. The ranking of input variables was evaluated based on the variables with high correlations.

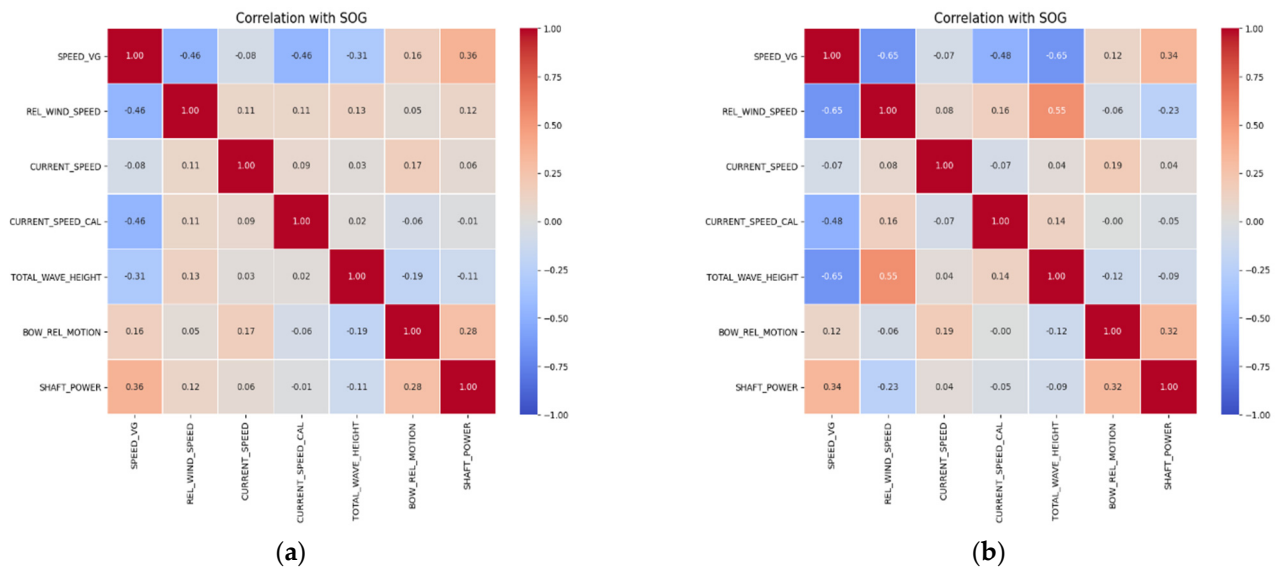


Figure 6. Correlation matrix of six input variables for SOG: (a) ballast condition; (b) laden condition.

#### 4.3. Selection of Independent Variable Using Coherence Function

The proposed model aims to predict the extent of the influence on speed performance by sequentially excluding the impact of other variables included in the input. Therefore, the order of input variables is crucial. To determine the order of input variables, the ordinary coherence (the contribution between input and output) was evaluated. After excluding the variables with low correlation, the contribution evaluation results for the remaining four variables according to Equation (9) are shown in Table 4.

$$r_{xy}^2 = \frac{|G_{xy}(f)|^2}{G_{xx}(f)G_{yy}(f)} \tag{9}$$

Based on the coherence analysis results, the order of input variables is as follows: “Current Speed—Shaft Horsepower (SHP)—Wave Height—Relative Wind Speed”. However, it was decided to exclude the variable “Shaft Horsepower”. In ideal conditions, any change in the shaft horsepower should give rise to speed change according to the speed–power curve, thereby making the coherence value near unity. In other words, the shaft power is considered to be input for the voluntary speed adjustment. However, the low coherence values around 0.1 between the SHP and the SOG imply that the SHP fluctuations measured

in real operation are essentially irrelevant measurement noise that can hardly result in speed change. The main engines of the ships are operated predominantly at constant power mode, which also makes it irrelevant to consider the SHP fluctuations. It is also worthwhile to mention that the relevant inputs for this study are the environmental disturbances that give rise to involuntary speed drop through added resistance. Consequently, the final order of input variables and their rankings are as follows: “Current Speed—Wave Height—Relative Wind Speed.” When the determined input variables are applied to Equation (1), the proposed ship’s performance prediction model (three inputs/single output) is represented as Equation (10). The values on the right-hand side represent the speed variations caused by each external force.

$$Y(f) = L_{1y}X_1(current) + L_{2y}X_{2.1}(wave) + L_{3y}X_{3.2i}(wind) + N \tag{10}$$

**Table 4.** Values of ordinary coherence functions.

Draft	Voyage	rel. Wind Speed	Wave Height	SHP	Current Speed_CAL (=STW – SOG)
Ballast	65	0.072	0.174	0.204	0.256
	66	0.065	0.209	0.170	0.266
	67	0.040	0.068	0.096	0.332
	68	0.039	0.044	0.060	0.308
	69	0.096	0.165	0.168	0.276
	70	0.045	0.095	0.127	0.156
	71	0.048	0.145	0.103	0.212
	Average 65~71	0.058	0.129	0.133	0.258
Laden	65	0.054	0.162	0.116	0.290
	67	0.042	0.083	0.079	0.451
	68	0.032	0.055	0.056	0.338
	69	0.032	0.070	0.073	0.387
	70	0.074	0.162	0.095	0.291
	Average 65~70	0.047	0.106	0.084	0.351

Figure 7, a graphical representation of Equation (10), illustrates the differences between the proposed MISO model and ISO 19030. Here, the total speed drop corresponds to  $Y(f)$  in Equation (10). The ISO 19030 standard compensates only for speed reduction caused by wind, while the MISO model sequentially eliminates speed reductions due to currents, waves, and wind based on the order determined by the contribution of input variables.

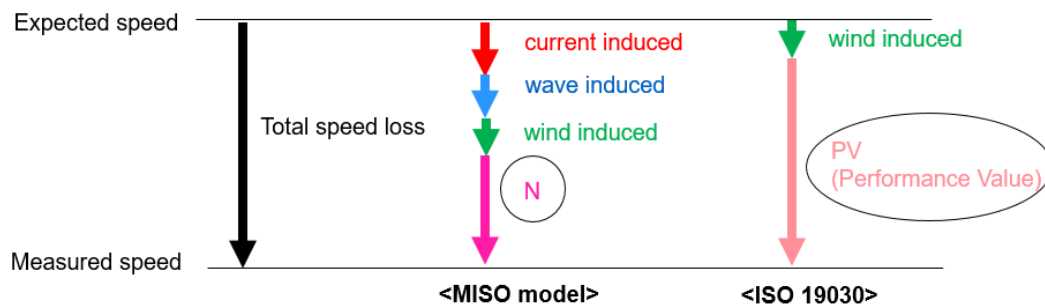


**Figure 7.** Comparison of the present dynamic MISO model and ISO 19030.

During the analysis of the entire navigation data, the frequency characteristics of each variable are used for Fourier transformation. To perform the Fourier transformation, the entire data is divided into  $2^n$  variable blocks. Initially, the variable block size was considered for a single-input single-output (SISO) model, and it was found to converge with 1024 blocks ( $2^{10}$ ) or more. Therefore, the data were divided into 1024 blocks, each containing data points from 10 s at 10 s intervals, resulting in a total duration of 10,240 s. Each variable is defined as the fluctuation (deviation) from the mean value in each block. By finding the optimal linear transfer function ( $L_{iy}$ ) between the input variables and the output, the proposed model sequentially removes the influence of each external force while examining the speed variation for each variable.

### 5. Results of Speed Performance Analysis Using MISO Model

#### 5.1. Behavior of Speed Performance with Respect to Voyage

In ISO 19030, the principal value (PV), which is a measure of the speed loss in real operation, can be calculated at every time instant. Similarly, the present Dynamic MISO model is capable of predicting the speed loss components at every time instant by means of Equation (10). Due to the vast amount of data and the highly stochastic nature, it is often convenient to take the average of such instantaneous speed loss over the entire time duration of each voyage. The resulting speed losses with respect to voyage pertaining to each input variable (external force) are listed in Tables 5 and 6 for the ballast condition and the laden condition, respectively. The corresponding graphs are presented in Figures 8 and 9. The total losses represent the difference between the expected speed based on the operation horsepower and the actual measured speed, for each voyage. They also provide information on how the three external forces influenced the total loss. The N-loss, obtained after excluding the effects of each external force, represents the non-linear impact, such as fouling.

**Table 5.** Speed loss percentage for input variables—ballast condition.

Draft	Voyage	Expected Speed [knots]	Measured Speed [knots]	Total Loss [knots]	X1 Loss (Current) [%]	X2 Loss (Wave Height) [%]	X3 Loss (rel. Wind Speed) [%]	N-Loss (Fouling, Aging) [%]
Ballast (second service)	40	16.195	15.574	0.621 (0.38%)	0.98	0.31	0.22	2.33
	41	14.847	14.159	0.688 (4.63%)	1.08	0.33	0.24	2.98
	42	15.553	14.675	0.878 (5.65%)	1.21	0.33	0.25	3.86
	43	14.093	13.498	0.595 (4.22%)	1.08	0.31	0.21	2.63
	44	13.961	13.088	0.873 (6.25%)	1.01	0.35	0.24	4.65
	46	14.617	14.070	0.547 (3.74%)	0.98	0.36	0.22	2.19
	47	13.874	13.278	0.596 (4.30%)	0.99	0.32	0.25	2.74
	49	15.634	14.078	1.556 (9.95%)	0.93	0.28	0.10	8.65
	50	15.481	15.096	0.385 (2.49%)	1.03	0.26	0.13	1.07
	51	13.954	13.318	0.636 (4.56%)	1.04	0.32	0.14	3.06
	52	15.435	14.872	0.563 (3.65%)	1.02	0.25	0.17	2.22
	53	15.444	14.497	0.947 (6.13%)	1.02	0.25	0.17	4.70
	54	15.454	14.646	0.808 (5.23%)	1.05	0.25	0.16	3.77
	55	15.826	15.272	0.554 (3.50%)	0.99	0.16	0.13	2.22
	60	15.579	14.310	1.269 (8.15%)	1.17	0.38	0.19	6.41
	61	15.856	14.594	1.262 (7.96%)	1.08	0.22	0.16	6.50
62	15.677	14.792	0.885 (5.65%)	1.10	0.24	0.13	4.17	
63	15.597	14.528	1.069 (6.85%)	1.07	0.24	0.13	5.40	

Table 5. Cont.

Draft	Voyage	Expected Speed [knots]	Measured Speed [knots]	Total Loss [knots]	X1 Loss (Current) [%]	X2 Loss (Wave Height) [%]	X3 Loss (rel. Wind Speed) [%]	N-Loss (Fouling, Aging) [%]
Ballast (third service)	65	14.052	13.372	0.680 (4.84%)	2.05	0.77	0.68	1.34
	66	15.158	14.628	0.530 (3.50%)	1.81	0.57	0.55	0.57
	67	14.589	13.659	0.930 (6.37%)	1.29	0.40	0.42	4.26
	68	15.394	13.244	2.150 (14.0%)	1.10	0.32	0.31	12.23
	69	15.065	13.087	1.978 (13.1%)	1.38	0.52	0.50	10.73
	70	14.840	14.462	1.378 (9.29%)	1.42	0.67	0.53	6.66
	71	14.454	12.370	2.084 (14.4%)	1.47	0.64	0.50	11.81
	72	14.062	12.670	1.392 (9.90%)	1.43	0.59	0.43	7.45
	73	13.837	12.783	1.054 (7.62%)	1.52	0.52	0.40	5.17
	74	14.072	12.675	1.397 (9.93%)	1.32	0.45	0.39	7.76
	75	14.335	12.164	2.171 (15.1%)	1.27	0.40	0.29	13.18
	76	14.140	11.845	2.295 (16.2%)	0.13	0.57	0.41	15.12
	77	13.935	11.974	1.961 (14.1%)	1.50	0.68	0.50	11.39

Table 6. Speed loss percentage for input variables—laden condition.

Draft	Voyage	Expected Speed [knots]	Measured Speed [knots]	Total Loss [knots]	X1 Loss (Current) [%]	X2 Loss (Wave Height) [%]	X3 Loss (rel. Wind Speed) [%]	N-Loss (Fouling, Aging) [%]
Laden (second service)	39	14.684	14.14	0.540 (3.68%)	0.99	0.54	0.38	1.76
	40	13.890	13.184	0.706 (5.08%)	1.14	0.26	0.33	3.35
	41	14.624	14.047	0.577 (3.95%)	1.16	0.18	0.59	2.02
	42	13.412	12.727	0.685 (5.11%)	0.94	0.35	0.27	3.55
	43	13.164	12.634	0.530 (4.03%)	1.00	0.32	0.26	2.45
	46	14.024	13.311	0.713 (5.08%)	1.03	0.35	0.25	3.46
	47	14.124	13.143	0.981 (6.95%)	0.98	0.23	0.22	5.52
	49	13.767	13.253	0.514 (3.73%)	1.22	0.24	0.14	2.14
	50	13.630	12.756	0.874 (6.41%)	1.19	0.32	0.14	4.77
	51	14.164	13.352	0.812 (5.73%)	1.09	0.30	0.17	4.17
	52	14.006	12.915	1.091 (7.79%)	1.04	0.24	0.16	6.35
	53	14.055	13.577	0.478 (3.40%)	1.10	0.24	0.14	1.93
	54	14.105	12.881	1.224 (8.68%)	1.06	0.23	0.13	7.26
	59	13.764	12.609	1.155 (8.39%)	0.96	0.23	0.16	7.04
	60	14.083	13.624	0.459 (3.26%)	1.13	0.19	0.14	1.80
	61	14.025	13.504	0.521 (3.71%)	1.01	0.26	0.14	2.30
62	14.086	12.729	1.357 (9.63%)	1.04	0.24	0.11	8.24	
63	14.056	12.944	1.112 (7.91%)	1.05	0.22	0.12	6.52	

Table 6. Cont.

Draft	Voyage	Expected Speed [knots]	Measured Speed [knots]	Total Loss [knots]	X1 Loss (Current) [%]	X2 Loss (Wave Height) [%]	X3 Loss (rel. Wind Speed) [%]	N-Loss (Fouling, Aging) [%]
Laden (third service)	65	13.836	13.089	0.747 (5.40%)	1.50	0.51	0.35	2.70
	67	14.077	12.622	1.455 (10.34%)	1.17	0.32	0.22	8.24
	68	14.009	12.898	1.111 (7.93%)	1.02	0.42	0.29	3.48
	69	13.881	13.204	0.677 (4.88%)	1.37	0.50	0.32	2.29
	70	13.648	11.368	2.280 (16.7%)	1.41	0.75	0.47	8.02
	71	13.481	10.825	2.656 (19.7%)	1.16	0.90	0.65	5.96
	72	13.957	12.739	1.218 (8.73%)	1.23	0.34	0.37	6.41
	73	13.599	12.609	0.990 (7.28%)	1.29	0.38	0.33	5.08
	74	12.878	11.337	1.541 (12.0%)	1.22	0.39	0.38	10.15
	76	13.384	12.028	1.356 (10.1%)	1.41	0.50	0.35	7.63
	77	13.753	12.384	1.369 (9.95%)	1.36	0.38	0.34	7.18

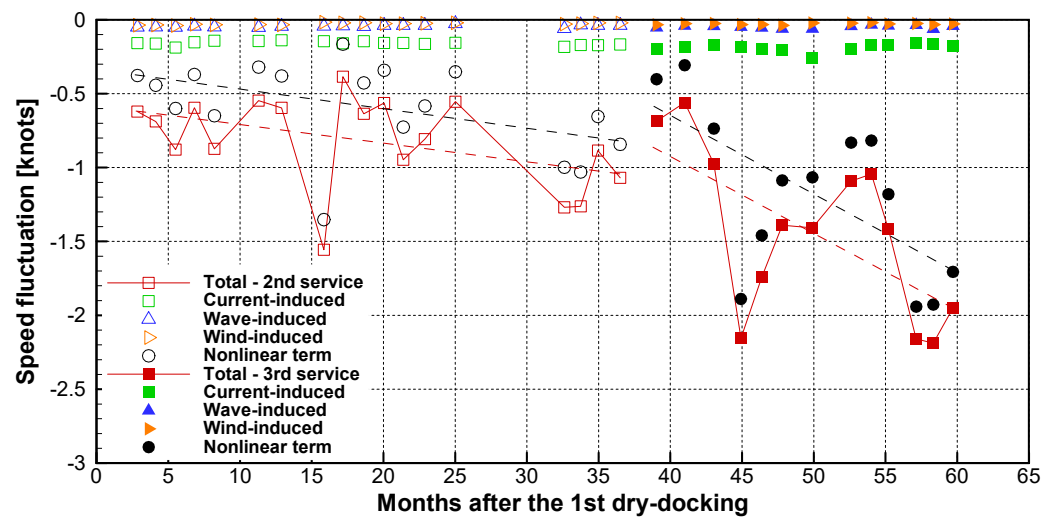


Figure 8. Speed fluctuation for input variables—ballast condition.

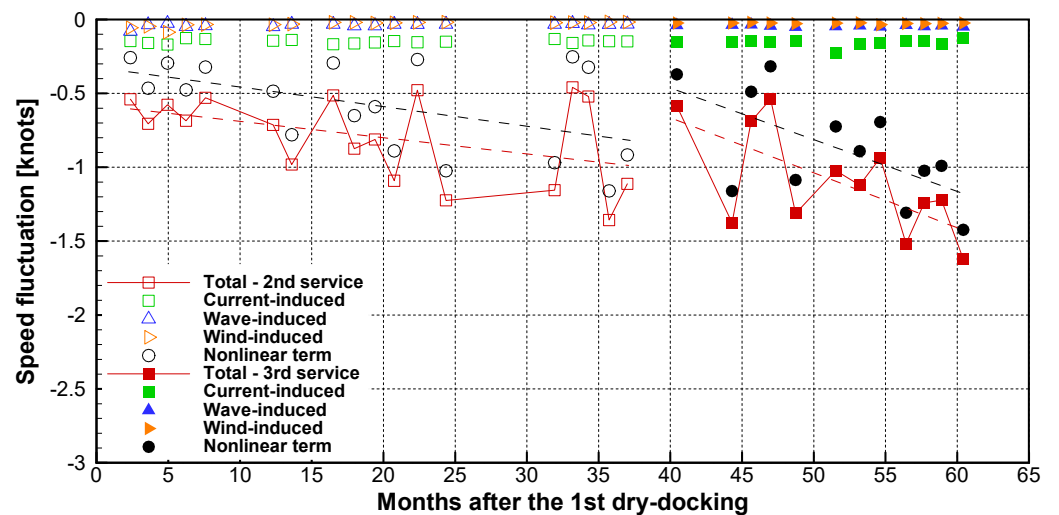


Figure 9. Speed fluctuation for input variables—laden condition.

5.2. Comparison with ISO 19030 Standard Analysis Results

The results of the present model, represented by the N-loss values, were compared with the performance values (PV) from the ISO 19030 standard. These values represent the speed loss after compensating for the proposed external forces in each model. The comparisons are shown in Figures 10 and 11; the red dotted lines represent the results from the ISO 19030 standard, while the black solid lines represent the results from the MISO model. The PV values from the ISO 19030 standard, which only compensate for the increase in resistance due to wind, show a nearly constant deviation of about 5% when compared to the N-loss values, which include compensation for all three forces (wind, waves, and currents). This indicates that the approximately 5% speed loss difference can be attributed to differences in speed correction due to waves and currents. This trend is observed for both ballast and laden conditions.

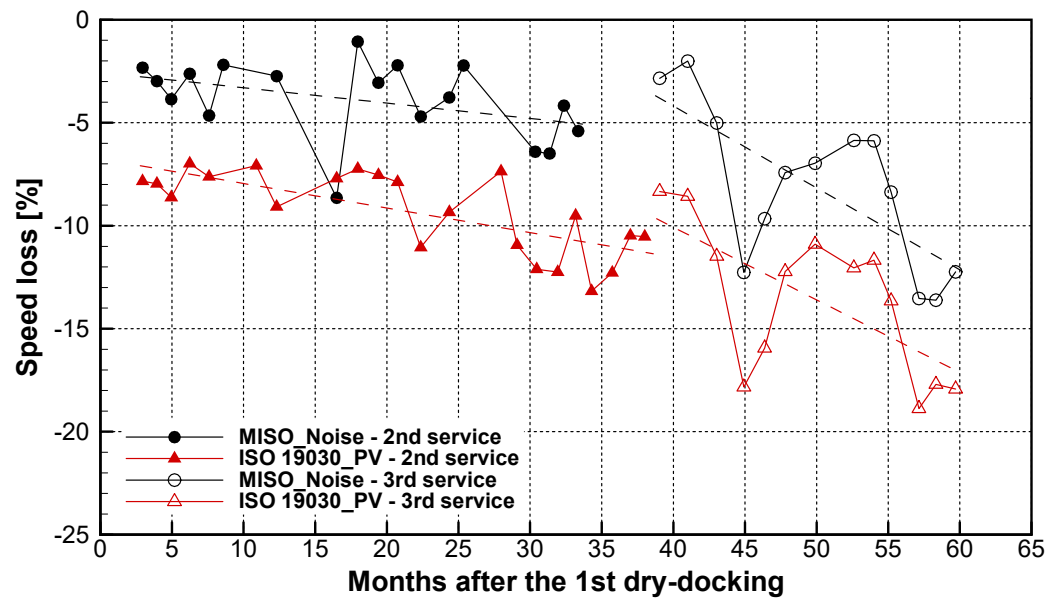


Figure 10. Prediction model verification with ISO 19030 Standard; comparison of speed loss [%] for each voyage—ballast condition.

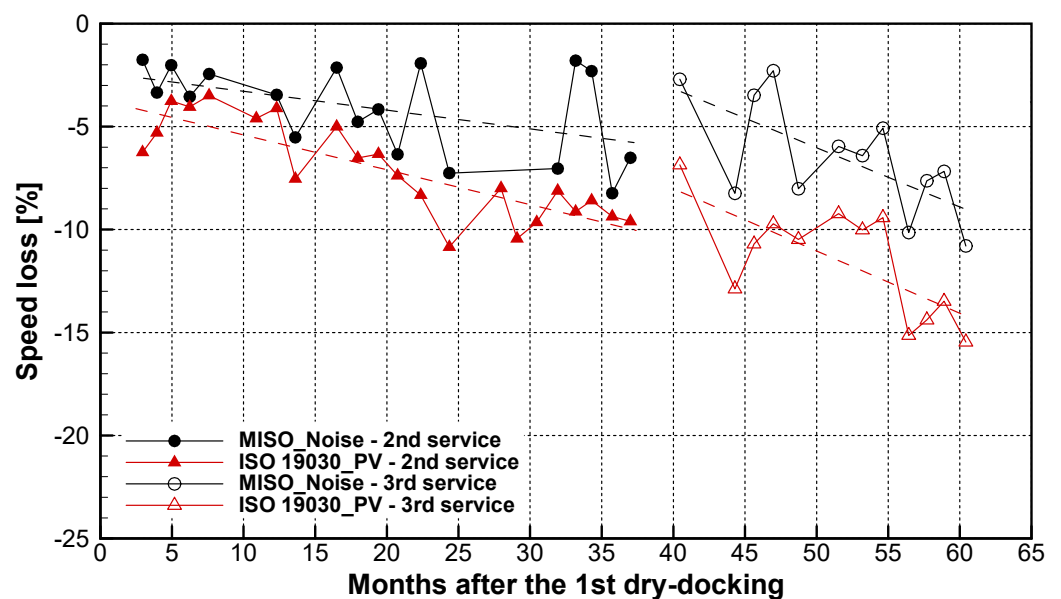


Figure 11. Prediction model verification with ISO 19030 Standard; comparison of speed loss [%] for each voyage—laden condition.

### 5.3. Comparison of Speed–Power Curves

Comparison of the speed–power curves for the original navigation data, ISO 19030 standard, and MISO model interpretation was performed. The reference speed–power curves are based on model test results and defined in the form of a power law equation as shown in Equation (11). The coefficients A and B for ballast conditions are 3.492 and 0.764, respectively, while for laden conditions, they are 3.16 and 2.725, respectively. The speed–power curves of the ISO 19030 standard method and MISO model were calculated by assuming a curve that shifts the original speed–power curve by an amount as shown in Equation (12), to minimize the mean square error (MSE).

$$Power = BV^A \tag{11}$$

$$Power = B(V - V_0)^A \tag{12}$$

For each voyage, we calculated the  $R^2$  (Equation (13)) and mean absolute percentage error (MAPE, (Equation (14))), comparing the predicted values with the actual values. The sum of squares error (SSE) represents the difference between the measured and predicted values, the sum of squares due to regression (SSR) represents the difference between the predicted values and the mean, and the sum of squares total (SST) represents the difference between the observed values and the mean. The results for the ballast draft and the laden draft are plotted in Figure 12a,b, respectively. In all voyages, the present MISO model led to a significant improvement in prediction accuracy over the ISO 19030. This improvement is even more remarkable for the laden draft cases.

$$R^2 = 1 - \frac{\sum_{i=1}^N (P_i^{predicted} - P_i^{actual})^2}{\sum_{i=1}^N (P_i^{predicted} - \bar{P})^2} = 1 - \frac{SSE}{SST} = \frac{SSR}{SST} \tag{13}$$

$$MAPE = \frac{100}{N} \times \sum_{i=1}^N \left| \frac{P_i^{predicted} - P_i^{actual}}{P_i^{predicted}} \right| \tag{14}$$

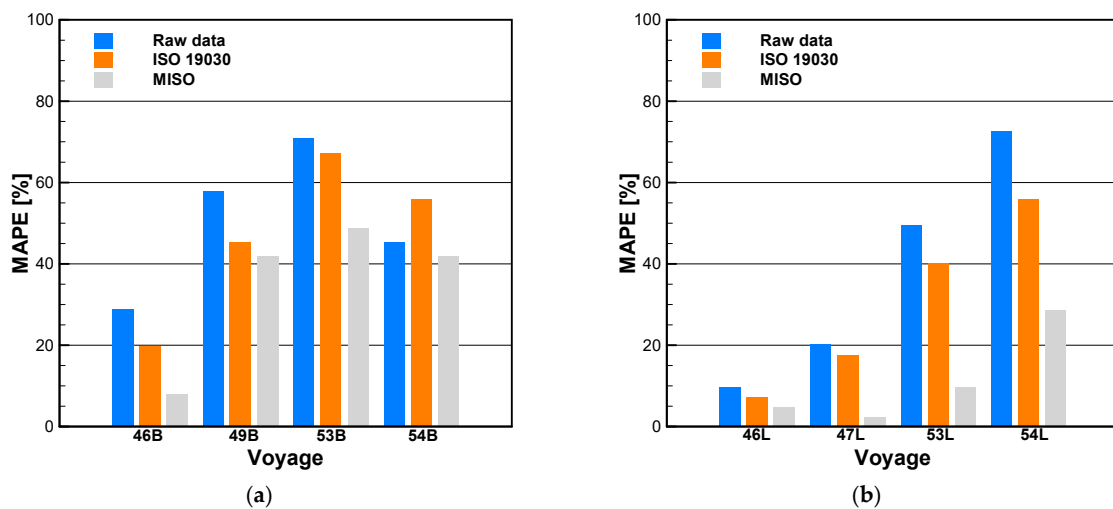


Figure 12. Comparison of MAPE (%) with model test: (a) ballast condition; (b) laden condition.

Figure 13 provides a clear illustration of the external force corrections based on the ISO 19030 standard and the MISO model, as explained in Figure 9. There are plotted four graphs, each of which corresponds to the individual voyage either in ballast draft (Figure 13a) or laden draft (Figure 13b). The symbol in the graph denotes each operational speed–power data, which is colored blue (raw data), red (ISO 19030), and green (MISO). At first sight, a significant scatter of blue symbols (raw data) is noted. This is a commonly

observed feature in the literature [22] and is associated with the random nature of external marine forces. The red symbols obtained from ISO 19030 still have a considerable degree of scatter. This implies that ISO 19030 seldom provides the correction of each speed–power datum except the filtering capability. However, it is remarkable that the green symbols by the present MISO model exhibit much smaller scatter in all voyages of Figure 13. It is noteworthy that the MISO model did not adopt filter preprocessing, which is used in the ISO 19030. Instead, the inputs and output were rectified by an optimal linear transfer function. The reduced extent of data scatter proves that such correction was effective to identify more reliable speed–power relationships in real operating conditions.

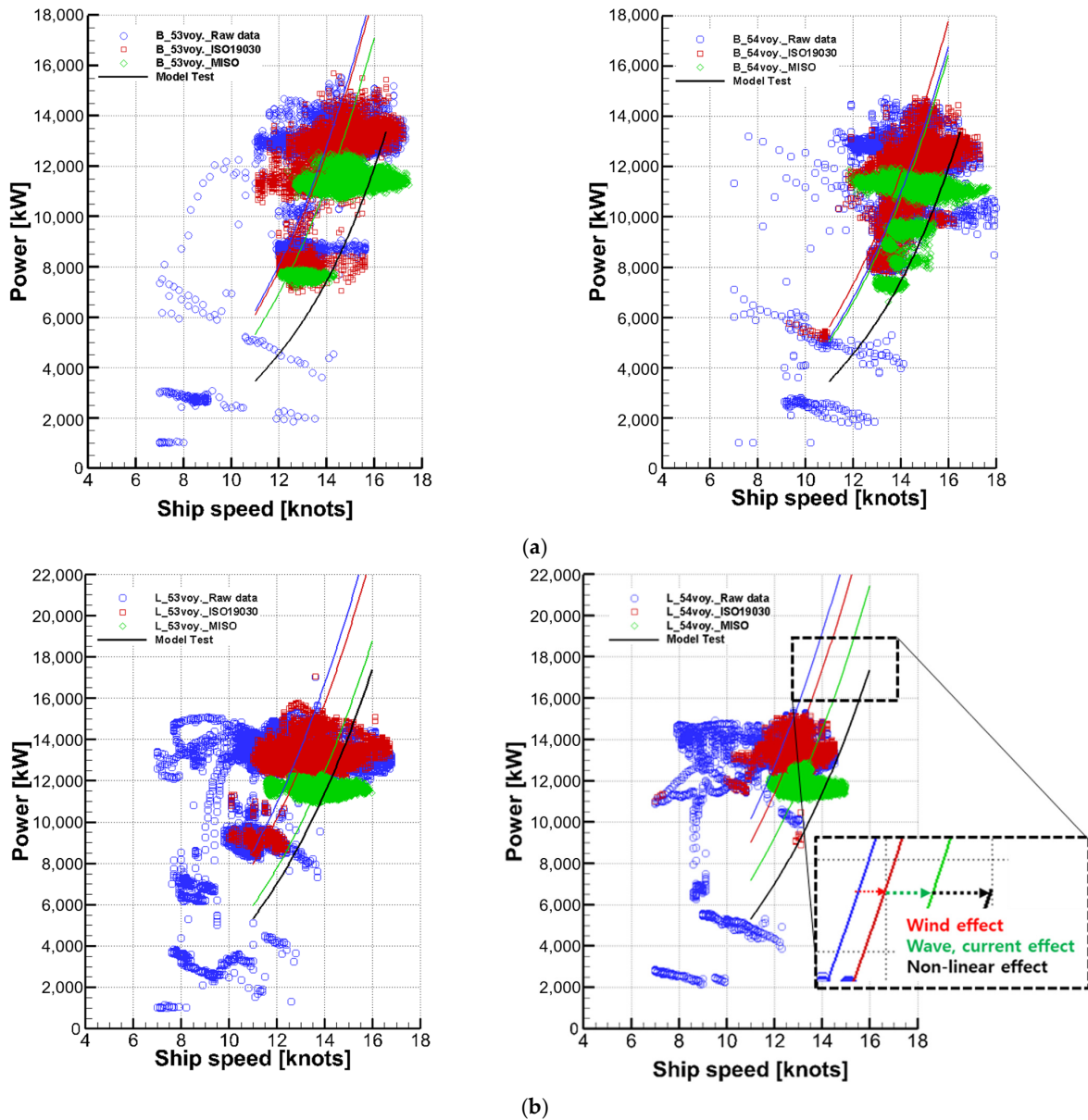


Figure 13. Comparison of the speed power curve: (a) ballast condition; (b) laden condition.

The solid curve in the same color represents the least-square fit in Equation (12) to the same colored symbols. As described earlier, the horizontal shift of the fitted speed–power curve  $V_0$  was determined to minimize the MSE between the data points and the fitted curve. Also, it can be regarded as the estimated speed drop from the respective correction method. The values were adjusted to achieve the minimum MSE and shift the speed–power curve. When corrected for wind resistance from the blue original data, it

becomes the red ISO 19030 standard analysis. Further correction for wave and current resistance results in the green MISO model analysis. Finally, when non-linear factors such as fouling are compensated for, the speed–power curve aligns with the speed–power curve from the ship design stage’s model tests. The ISO 19030 method only corrects for wind resistance, allowing us to observe the speed degradation trend of a specific ship. The MISO model corrects for all three external forces (wind, waves, and current resistance), making it possible to conduct further supplementary research. It is possible to compare the operational performances of different vessels based on the present MISO model.

5.4. Time Delays between Environmental Disturbances and Speed Response

The speed–power curves of the ISO 19030 standard method and MISO model were calculated by assuming a curve that shifts the original speed–power curve by an amount as shown in Equation (12), to minimize the mean square error (MSE). The MISO model was designed based on the assumption that changes in external forces lead to an increase in resistance, resulting in speed variations. Additionally, the model takes into consideration the time delay (time delay,  $\tau_0$ ) in the frequency characteristics of the target vessel, which may vary depending on its size and type. This dynamic modeling approach distinguishes it from traditional static performance prediction models used in previous research. The MISO model predicts time delays for each external force, making it a dynamic model capable of capturing the temporal effects of different forces on the speed of the vessel.

Figure 14 shows the results of the ship’s speed and time delay (phase shift) for each external force (wind, waves, and currents). It is observed that there is a specific time delay for each external force regardless of the voyage, i.e., approximately 40 s for wave, 7 s for current, and almost zero for wind. This confirms that the initial assumption of the proposed prediction model, which considers dynamic effects during ship operation, is valid.

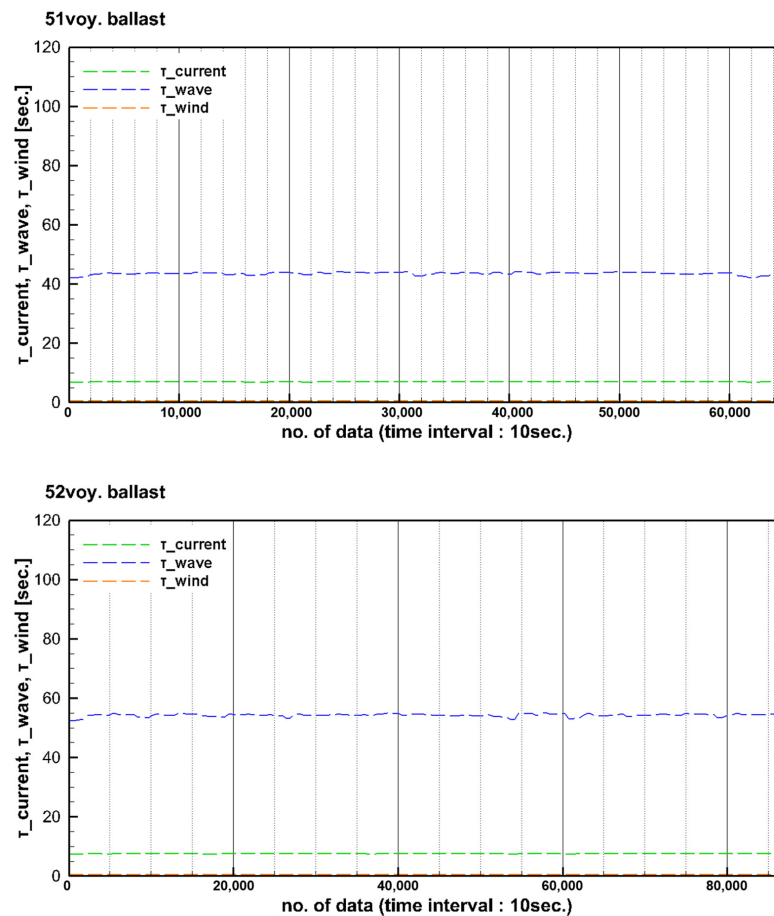


Figure 14. Prediction of time constants for three external forces.

## 6. Discussions

Analyzing the results of the present predictive model, the speed variations based on input variables show relatively consistent patterns across different voyages. This is attributed to the fact that the ship operates on the same route and experiences similar external forces for each voyage. Both total loss and N-loss exhibit similar trends, indicating that the primary factor influencing speed loss is noise, such as fouling. Furthermore, comparing the N-loss component of the predictive model with the performance values (PV) from the ISO 19030 standard, the two predictive models exhibited a consistent trend with a steady deviation (attributed to additional resistance from waves and currents). It is noteworthy that the present MISO model contributed to a significant reduction in the data scatter of the speed–power relationship, thereby enhancing the reliability of the evaluation of the in-service speed performance of the ship. Consequently, this MISO model could potentially enable performance comparison between different vessels during operations, which has not been the case with the conventional ISO 19030 standard.

As pointed out in the introduction, there have been proposed many energy-saving methods for ships. Such energy-saving methods can be retrofitted to existing ships, and it becomes necessary to assess the energy-saving efficiency between ships through the performance comparison between vessels with and those without energy-saving methods. The afore-mentioned advantage of MISO model can be particularly notable in this regard.

## 7. Conclusions

In order to respond to the environmental regulations of the International Maritime Organization (IMO) and to ensure competitive ship operation management, accurate prediction of performance changes in actual operating conditions is crucial. Currently, the ISO 19030 standard method is widely used for the interpretation of actual operating performance. In addition, various research efforts are underway to achieve precise predictions. However, there is a need for improvement in terms of clarifying input/output variables based on dynamic relationships and addressing the necessity for enhancements due to excessive data filtering. In this study, we propose a predictive model for operational performance to improve existing performance prediction models and the ISO 19030 standard. In actual operations, variations in external factors such as relative wind speed and wave conditions lead to increased resistance from wind and waves, resulting in speed fluctuations. During such scenarios, it is assumed that there are specific time delays based on the ship's size and type, along with corresponding frequency characteristics. Based on these assumptions, we modeled the unknown frequency characteristics as a multi-input single-output system to evaluate the influence of each external force on speed performance. The characteristics of the proposed predictive model are as follows:

- No additional filtering is applied beyond removing outliers caused by mechanical faults in the data.
- Correlations between various variables and the ship's speed performance are evaluated to determine input variables.
- The optimal transfer functions between environmental disturbances and the speed fluctuations have been derived to identify the dynamic response characteristics of the ship.
- The impact of speed variation due to first-level input variables is assessed first, then, other variables are sequentially evaluated by excluding the influence of the preceding ones.

A closer inspection of the speed–power data given in Figure 13 reveals the superiority of the present MISO model over the existing ISO 19030 standard in that it gives better collapse to the underlying physics of the speed–power curve. However, the present MISO model has its own limit of a linear model, which is not consistent with the nonlinear nature of speed–power curve. Although this limit can be alleviated by the linearization technique employed in this study, there still remains unresolved issue of non-linearity. The nonlinear regression capability of a neural network can make it a relevant candidate to tackle this

issue. The grey-box approach, which combines the present dynamic linear MISO model and a neural network, is considered to be the topic of future research.

**Author Contributions:** Conceptualization, I.L.; methodology, Y.C.; software, Y.C.; validation, I.L.; formal analysis, Y.C.; investigation, Y.C.; resources, I.L.; data curation, Y.C.; writing—original draft preparation, Y.C.; writing—review and editing, I.L.; visualization, Y.C.; supervision, I.L.; project administration, I.L.; funding acquisition, I.L. All authors have read and agreed to the published version of the manuscript.

**Funding:** This work was supported by a grant from the National Research Foundation of Korea (NRF) funded by the Ministry of Science and ICT of Korea (No. 2022R1A2C2010821), by the “Regional Innovation Strategy (RIS)” through the National Research Foundation of Korea (NRF) funded by the Ministry of Education (Grant No. 2023RIS-007), and by BK21 FOUR Graduate Program for Green-Smart Naval Architecture and Ocean Engineering of Pusan National University.

**Institutional Review Board Statement:** Not applicable.

**Informed Consent Statement:** Not applicable.

**Data Availability Statement:** The data that support the findings of this study are available from the corresponding author upon reasonable request.

**Conflicts of Interest:** The authors declare no conflicts of interest.

## References

- Merlo, S.; Gabarrell Durany, X.; Pedroso Tonon, A.; Rossi, S. Marine Microalgae Contribution to Sustainable Development. *Water* **2021**, *13*, 1373. [[CrossRef](#)]
- Barreiro, J.; Zaragoza, S.; Diaz-Casas, V. Review of Ship Energy Efficiency. *Ocean Eng.* **2022**, *257*, 111594. [[CrossRef](#)]
- Handayani, M.P.; Kim, H.; Lee, S.; Lee, J. Navigating Energy Efficiency: A Multifaceted Interpretability of Fuel Oil Consumption Prediction in Cargo Container Vessel Considering the Operational and Environmental Factors. *J. Mar. Sci. Eng.* **2023**, *11*, 2165. [[CrossRef](#)]
- Chen, Z.S.; Lam, J.S.L.; Xiao, Z. Prediction of Harbour Vessel Fuel Consumption Based on Machine Learning Approach. *Ocean Eng.* **2023**, *278*, 114483. [[CrossRef](#)]
- Fan, A.; Yang, J.; Yang, L.; Wu, D.; Vladimir, N. A Review of Ship Fuel Consumption Models. *Ocean Eng.* **2022**, *264*, 112405. [[CrossRef](#)]
- Zhou, T.; Hu, Q.; Hu, Z.; Zhen, R. An Adaptive Hyper Parameter Tuning Model for Ship Fuel Consumption Prediction under Complex Maritime Environments. *J. Ocean Eng. Sci.* **2022**, *7*, 255–263. [[CrossRef](#)]
- Zhang, M.; Tsoulakos, N.; Kujala, P.; Hirdaris, S. A Deep Learning Method for the Prediction of Ship Fuel Consumption in Real Operational Conditions. *Eng. Appl. Artif. Intell.* **2024**, *130*, 107425. [[CrossRef](#)]
- Poulsen, R.T.; Viktorelius, M.; Varvne, H.; Rasmussen, H.B.; von Knorring, H. Energy Efficiency in Ship Operations—Exploring Voyage Decisions and Decision-Makers. *Transp. Res. Part D Transp. Environ.* **2022**, *102*, 103120. [[CrossRef](#)]
- Durluk, I.; Miller, T.; Cembrowska-Lech, D.; Krzemińska, A.; Złoczowska, E.; Nowak, A. Navigating the Sea of Data: A Comprehensive Review on Data Analysis in Maritime IoT Applications. *Appl. Sci.* **2023**, *13*, 9742. [[CrossRef](#)]
- Lang, X.; Mao, W. A semi-empirical model for ship speed loss prediction at head sea and its validation by full-scale measurements. *Ocean Eng.* **2020**, *209*, 107494. [[CrossRef](#)]
- Tilling, F.; Ringsberg, J.W. A 4 DOF simulation model developed for fuel consumption prediction of ships at sea. *Ships Offshore Struct.* **2019**, *14* (Suppl. 1), 112–120. [[CrossRef](#)]
- Kim, Y.R.; Steen, S.; Kramel, D.; Muri, H.; Strømman, A.H. Modelling of ship resistance and power consumption for the global fleet: The MariTEAM model. *Ocean Eng.* **2023**, *281*, 114758. [[CrossRef](#)]
- Yan, R.; Wang, S.; Psaraftis, H.N. Data analytics for fuel consumption management in maritime transportation: Status and perspectives. *Transport. Res. E Logist. Transport. Rev.* **2021**, *155*, 102489. [[CrossRef](#)]
- Huang, L.; Pena, B.; Liu, Y.; Anderlini, E. Machine learning in sustainable ship design and operation: A review. *Ocean Eng.* **2022**, *266*, 112907. [[CrossRef](#)]
- Petersen, J.P.; Winther, O.; Jacobsen, D.J. A Machine-Learning Approach to Predict Main Energy Consumption under Realistic Operational Conditions. *Ship Technol. Res.* **2012**, *59*, 64–72. [[CrossRef](#)]
- Shin, J.H.; Shim, J.Y.; Park, J.W.; Choi, D.H.; Byeon, S.S. A Study on the Improvement of Sailing Efficiency Using Big Data of Ship Operation. In Proceedings of the Korean Society of Marine Environment & Safety, Mokpo, Republic of Korea, 27–28 April 2017.
- Yoo, B.; Kim, J. Powering performance analysis of full-scale ships under environmental disturbances. *IFAC PapersOnLine* **2017**, *50*, 2323–2328. [[CrossRef](#)]
- Kim, D.H.; Han, S.J.; Jung, B.K.; Han, S.H.; Lee, S.B. A Machine Learning-Based Method to Predict Engine Power. *J. Korean Soc. Mar. Environ. Saf.* **2019**, *25*, 851–857. [[CrossRef](#)]

19. ISO 15016:2015(E); Ships and Marine Technology—Guideline for the Assessment of Speed and Power Performance by Analysis of Speed Trial Data. ISO: Geneva, Switzerland, 2015.
20. Karagiannidis, P.; Themelis, N.; Zaraphonitis, G.; Spandonidis, C.; Giordamlis, C. Ship Fuel Consumption Prediction using Artificial Neural Network. In Proceedings of the Hellenic Institute of Marine Technology—Annual Meeting 2019, Athens, Greece, 26–27 November 2019.
21. Wahl, J.M. Prediction of Fuel Consumption of a Ship in Transit Using Machine Learning. Master’s Thesis, Norwegian University of Science and Technology, Trondheim, Norway, 2019.
22. Uyanık, T.; Karatug, Ç.; Arslanoğlu, Y. Machine learning approach to ship fuel consumption: A case of container vessel. *Transport. Res. Part D-Transport. Environ.* **2020**, *84*, 102389. [[CrossRef](#)]
23. Gupta, P.; Rasheed, A.; Steen, S. Ship performance monitoring using machine-learning. *Ocean Eng.* **2022**, *254*, 111094. [[CrossRef](#)]
24. Abebe, M.; Shin, Y.; Noh, Y.; Lee, S.B.; Lee, I. Machine Learning Approaches for Ship Speed Prediction towards Energy Efficient Shipping. *Appl. Sci.* **2020**, *10*, 2325. [[CrossRef](#)]
25. Cho, Y.; Jeon, K.H.; Lee, S.B.; Park, H.; Lee, I. Evaluation of In-service Speed Performance Improvement by means of FDR-AF (Frictional Drag Reducing Anti-Fouling) marine coating based on ISO 19030 standard. *Sci Rep.* **2021**, *11*, 1062. [[CrossRef](#)] [[PubMed](#)]
26. Boychuk, I.P.; Grinek, A.V.; Martyushev, N.V.; Klyuev, R.V.; Malozyomov, B.V.; Tynchenko, V.S.; Kukartsev, V.A.; Tynchenko, Y.A.; Kondratiev, S.I. A Methodological Approach to the Simulation of a Ship’s Electric Power System. *Energies* **2023**, *16*, 8101. [[CrossRef](#)]
27. Zwierzewicz, Z.; Dorobczyński, L.; Jaszczak, S. Design of ship course-keeping system via active disturbance rejection control using a full-scale realistic ship model. *Procedia Comput. Sci.* **2021**, *192*, 3000–3009. [[CrossRef](#)]
28. ISO/TC8/SC2 ISO/DIS 19030-1; Ships and Marine Technology—Measurement of Changes in Hull and Propeller Performance—Part 1: General Principles. ISO: Geneva, Switzerland, 2016.
29. ISO/TC8/SC2 ISO/DIS 19030-2; Ships and Marine Technology—Measurement of Changes in Hull and Propeller Performance—Part 2: Default Method. ISO: Geneva, Switzerland, 2016.
30. Cho, Y.; Lee, I.; Jeon, K.H.; Lee, S.B. Frictional Resistance and Speed Performance Review based on Actual Operating data for 175k BC. In Proceedings of the 5th Hull Performance & Insight Conference (HullPIC 2020), Tullamore, Ireland, 26–28 October 2020.
31. Park, B.J.; Shin, M.S.; Ki, M.S.; Lee, G.J.; Lee, S.B. Experience in Applying ISO 19030 to Field Data. In Proceedings of the Second Hull Performance & Insight Conference (HullPIC 2017), Ulrichshusen, Germany, 27–29 March 2017; pp. 150–155.
32. Bendat, J.S.; Piersol, A.G. *Random Data: Analysis and Measurement Procedures*, 3rd ed.; Wiley: Hoboken, NJ, USA, 2000; pp. 240–259.

**Disclaimer/Publisher’s Note:** The statements, opinions and data contained in all publications are solely those of the individual author(s) and contributor(s) and not of MDPI and/or the editor(s). MDPI and/or the editor(s) disclaim responsibility for any injury to people or property resulting from any ideas, methods, instructions or products referred to in the content.